



Non-invasive phenotyping for water and nitrogen uptake by deep roots explored using machine learning

Satyasaran Changdar · Olga Popovic · Tomke Susanne Wacker ·
Bo Markussen · Erik Bjørnager Dam · Kristian Thorup-Kristensen

Received: 21 February 2023 / Accepted: 22 August 2023 / Published online: 6 September 2023
© The Author(s) 2023

Abstract

Background and aims Root distribution over the soil profile is important for crop resource uptake. Using machine learning (ML), this study investigated whether measured square root of planar root length density (Sqrt_pRLD) at different soil depths were related to uptake of isotope tracer (^{15}N) and drought stress indicator (^{13}C) in wheat, to reveal root function.

Methods In the RadiMax semi-field root-screening facility 95 winter wheat genotypes were phenotyped for root growth in 2018 and 120 genotypes in 2019. Using the minirhizotron technique, root images were

acquired across a depth range from 80 to 250 cm in May, June, and July and RL was extracted using a convolutional neural network. We developed ML models to explore whether the Sqrt_pRLD estimates at different soil depths were predictive of the uptake of deep soil nitrogen - using deep placement of ^{15}N tracer as well as natural abundance of ^{13}C isotope. We analyzed the correlations to tracer levels to both a parametrized root depth estimation and an ML approach. We further analyzed the genotypic effects on root function using mediation analysis.

Results Both parametrized and ML models demonstrated clear correlations between Sqrt_pRLD distribution and resource uptake. Further, both models demonstrated that deep roots at approx. 150 to 170 cm depth were most important for explaining the plant content of ^{15}N and ^{13}C isotopes. The correlations were higher in 2018.

Conclusions The results demonstrated that, parametrized models and ML-based analysis provided complementary insight into the importance of deep rooting for water and nitrogen uptake.

Keywords Machine learning · Deep rooting · Deep resource uptake · Random forest · ^{13}C · ^{15}N

Responsible Editor: Andrea Schnepf.

Supplementary information The online version contains supplementary material available at <https://doi.org/10.1007/s11104-023-06253-7>.

S. Changdar (✉) · E. B. Dam
Department of Computer Science, Faculty of Science,
University of Copenhagen, Copenhagen, Denmark
e-mail: sach@di.ku.dk

S. Changdar · O. Popovic · T. S. Wacker ·
K. Thorup-Kristensen
Department of Plant and Environmental Sciences, Faculty
of Science, University of Copenhagen, Copenhagen,
Denmark

B. Markussen
Department of Mathematical Sciences, Faculty of Science,
University of Copenhagen, Copenhagen, Denmark

Abbreviations

pRLD	Planar root length density
RL	Root length
Sqrt_pRLD	Square root of planar root length density

D ₅₀	50% of the Sqrt_pRLD is accumulated
SI	Sigmoid inflection
ML	Machine learning
RF	Random forest
GB	Gradient boosting

Introduction

To achieve sustainable and climate resilient crop production, we need crops to have deep and well-developed root systems, enabling efficient use of resources also from deeper soil layers. One way to improve crop root systems is through breeding, but to do this efficient root phenotyping is required, allowing the measurement of the genetic component of variability in the relevant root traits. Root measurements are notoriously difficult, as roots and their uptake activity are hidden in the soil and difficult to observe. Therefore, a range of facilities have been developed for root phenotyping (Cai et al. 2016; Eberbach et al. 2013; Svane et al. 2019b), but there is a need for further development as well as for verification of the validity of the results obtained.

Water and nitrogen are important soil resources considered in crop production. Efficient crop water use is needed for productivity and resilience in dry periods. Efficient nitrogen use, particularly from deeper soil layers (Thorup-Kristensen and Kirkegaard 2016), is needed to reduce the need for nitrogen fertilizer input and to minimize nitrogen leaching loss to the environment. Water and nitrate are more mobile in the soil medium than most plant nutrients, meaning that in periods with surplus water supply, they tend to move downwards to deeper soil layers (Thorup-Kristensen and Kirkegaard 2016). Thus, deeper rooting will likely increase the ability of crops to take up water and nitrogen when needed, and help to recover the part of these resources at maximum risk of loss.

This leads to a need to develop root phenotyping methods, but also to verify that deeper rooted phenotypes actually lead to increased water and nitrate uptake from the soil. The RadiMax root phenotyping facility (Svane et al. 2019b) was developed specifically for such studies. Images of roots in the soil are obtained through minirhizotrons, and data for planar root length density (pRLD) on individual images are obtained using the AI based image analysis tool RootPainter (Smith et al. 2022). The facility and

experiments allow the use of isotope tracers as indicators of root activity, where we used deep injection of a ¹⁵N labelled isotope solution to study deep nitrogen uptake (Wacker et al. 2022). Natural abundance of ¹³C in grains was used to evaluate the genotypic potential for drought resilience. Due to natural isotope discrimination processes (Zhang et al. 2009), ¹³C composition could be used as an indicator for water stress as ¹³C concentration increase under water stress, leading to a less negative delta value.

The semi-automated root imaging process and use of fully automated deep learning for image analysis enable us to collect large amounts of root data containing information about root architecture. Using ML on these large datasets allows linking data from root images to root function and to maximize the information we can extract from the data.

Machine learning can be used to analyze hierarchical and non-linear relationships between predictor variables and response variables and this is often more effective than traditional linear regression methods (Baker et al. 2018). The size and quality of experimental multimodal data in agriculture are constantly growing. Thereby, ML offers potential for insight into complex agricultural relationships. Random Forests (RF) (Breiman 2001) is a widely used ML algorithm, that is known for allowing many variables with relatively small numbers of observations and in addition providing an assessment of variable importance (Breiman 2001; Ishwaran 2007; Strobl et al. 2007).

In soil science and hydrology, neural network models have been used extensively to estimate soil retention and hydraulic conductivity using a variety of easy-to-measure data (Pachepsky and Rawls 1999; Schaap and Leij 1998). Even though neural nets have become more popular in deep learning for image segmentation, and pattern recognition, they are less interpretable (Toms et al. 2020) as their complex structure and large number of parameters make it difficult to understand how they make decisions. Neural networks work by learning patterns in the data, and these patterns are represented in the connections between neurons, which are adjusted during the training process (Kiranyaz et al. 2021). As a result, it can be difficult to understand how specific input data is being processed and what features the model is using to make its predictions. Awika et al. (2021) employed machine learning techniques to examine the phenotypic and genetic correlations between root traits and

shoot fresh weights of different baby spinach accessions grown in small pots under low and high nitrogen concentrations.

While the root observations are dynamic and include data for different depth increments at different time points, the tracer data typically give one end point measurement at crop harvest, showing an integrated effect of roots at different depths over the crop growth period. Wacker et al. (2022) investigated deep root traits in winter wheat genotypes and their correlation with deep nitrogen (N) uptake using minirhizotron root imaging and ^{15}N tracer uptake analysis over two years. They identified deep root traits that predicted a portion of the tracer uptake variation, indicating the potential for breeding genotypes with enhanced deep N uptake capabilities.

The root images from the RadiMax facility were previously investigated. It was demonstrated that roots could be identified in the images using a deep learning-based method (Smith et al. 2020). This allowed estimation of Sqrt_pRLD for each individual image.

This study uses machine learning to investigate the following:

- Is estimated root depth related to water and nitrogen uptake?
- Does Sqrt_pRLD distribution across soil depths add additional understanding of root function?
- What is the genotypic contribution to the variation in root growth and function?

Materials and methods

Experimental systems

The RadiMax semi-field facility (Svane et al. 2019b) was designed for root phenotyping of crops grown in soil to maturity. In two experimental units, modern winter wheat cultivars and advanced breeding material were grown in two seasons, 2018 (95 winter wheat genotypes) and 2019 (120 winter wheat genotypes) (Wacker et al. 2022). The plants were sown at 300 plants m^{-2} density with 0.25 m row distance. Root imaging was performed with multi-spectral cameras (Svane et al. 2019a) through a minirhizotron system installed in the experimental units. The multispectral imaging technique has been used to

distinguish differences in young, older, and dead roots, as well as for robust discrimination of rhizosphere components, all based on differences in reflectance. Minirhizotron tubes (PMMA-Plastic) with 0.06 mm inner diameter and total length of 5.5 m were installed 0.4 m above sloping (23.5° slope) bottom of experimental unit and were used for root observations. Root imaging was done by RadiMax cameras (5 Mpx CMOS) at 5 wavelengths (405, 450, 590, 660, and 940 nm) in the visible-near-infrared region in $2448 \times 204 \times 5$ pixels resolution. Each camera is positioned to focus on the upper surface of MR tube, and each image covers an area of 20 cm^2 . The range of imaging was from 80 to 250 cm soil depth and images were taken every 3.5 cm soil depth.

Drought experiment

The RadiMax facility has the possibility to exclude rainwater via large rain-out shelters (Svane et al. 2019b). The rain-out shelters were used in both years from late May to maturity in July, creating a drought condition. The facility is equipped with a sub-surface irrigation system, which can be used to irrigate the crop with increasing soil depths. In 2018, the subsurface irrigation system was used from May onwards, creating water supply with increasing soil depths and in the beginning of July soil water content decreased to 12% VWC at 1 m soil depth. In 2019, the subsurface irrigation system was not used. In this year, the total soil water availability increased with depth. Despite the fact that subirrigation was not used in 2019, the drying of the soil profile was delayed when compared to 2018 and at 1 m soil depth in July VWC was 14%. In both years, water extraction has been observed at 2 m soil depth, with 22% VWC. At 2 m depth, soil temperature was higher (1°C) in 2018 than in 2019. More details on soil water supply in the experiment can be found in (Wacker et al. 2022, Fig. 4c-f).

Tracer injection and plant sampling

To study deep N uptake, an isotopic tracer of ^{15}N ($\text{Ca}^{15}\text{NO}_3)_2$, 98% enriched) was injected into the soil at 180 cm depth (Wacker et al. 2022) to all replicates at anthesis. Nitrogen isotope was injected using existing sub-irrigation dripline, perpendicular to the plant rows and MR tubes. At harvest, a sample (10

ears) corresponding to the aboveground area above the ^{15}N injection was taken (0.3 m^2 wide area), dried at $105\text{ }^\circ\text{C}$ for 48 h, milled and grains were analyzed for ^{15}N content via mass-spectroscopy (Wacker et al. 2022) and to study the indirect effect of deep-water uptake, the same sample was also analyzed for ^{13}C discrimination.

Root image analysis

Before image analysis, incomplete samples due to broken tubes or missing isotope data were identified and eliminated (16 tubes in 2018, 28 in 2019) from the dataset. The visible roots in each image were segmented using a convolutional neural network (Smith et al. 2020). For each image, the total length of segmented roots was extracted (Han et al. 2021), giving the RL. We then define the pRLD as the total root length in an image (cm) divided by the area of the image (cm^2). For robust statistical analysis and to avoid excessive influence from root-saturated images, we used the square root of the pRLD (Sqrt_pRLD) as our key quantification of root presence in each image. This is because water and N are relatively mobile resources in the soil, requiring a relatively low root density for efficient uptake. As root density increases, competition between the roots also increases, leading to a decrease in the uptake per unit root length. The unit of pRLD being cm^{-1} , the unit of Sqrt_pRLD becomes $\text{cm}^{-1/2}$.

Facility position correction

Planar root length density and isotope composition measurements showed strong position effects, mainly in one unit of the facility (Fig. 1) which may

have been caused by differences in soil compaction caused during the construction of the facility. Therefore, for all the analyses presented, the variables (isotopes measurements and Sqrt_pRLD) were linearly corrected for distance from the end of the facility. In other experiments (not reported), also piecewise linear corrections were used with very similar results.

Root distribution analysis

We investigated the influence of root distribution in two complementary ways. First, we defined parametrized models for estimation of the root depth, and analyzed their ability to predict isotope data.

Second, we defined a machine learning approach to investigate whether other aspects of the root distribution could contribute to explaining the root function indicated by the uptake of the isotope tracer ^{15}N enrichment and natural ^{13}C discrimination.

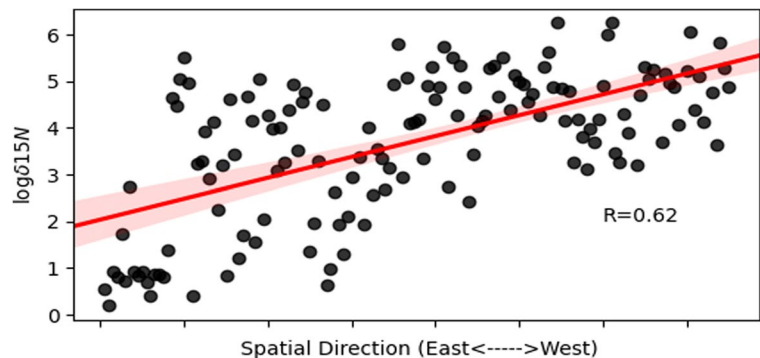
Root depth estimates

From minirhizotron image-based Sqrt_pRLD data, we designed estimates of the root depth for each position in the facility. In previous studies, root density has been modelled by an exponential model as a function of depth (Zuo et al. 2004) and we implemented that as a baseline comparison.

However, based on inspection of Sqrt_pRLD as a function of soil depth (example shown in Fig. 2), the sigmoid function appeared to fit the profiles better (Fig. 2, the goodness of fit $R^2 = 0.85$) and therefore potentially give a better estimator for root depth.

We fitted these two mathematical models to the Sqrt_pRLD measurements for each replicate in the facility using nonlinear regression (implemented

Fig. 1 The scatter diagram of $\log \delta^{15}\text{N}$ with regression line in one of the experimental units in 2018 is presented to illustrate the potential confounding effect. $\log \delta^{15}\text{N}$ was strongly correlated with position ($R = 0.62$). The shaded area represents the 95% confidence interval for the regression line



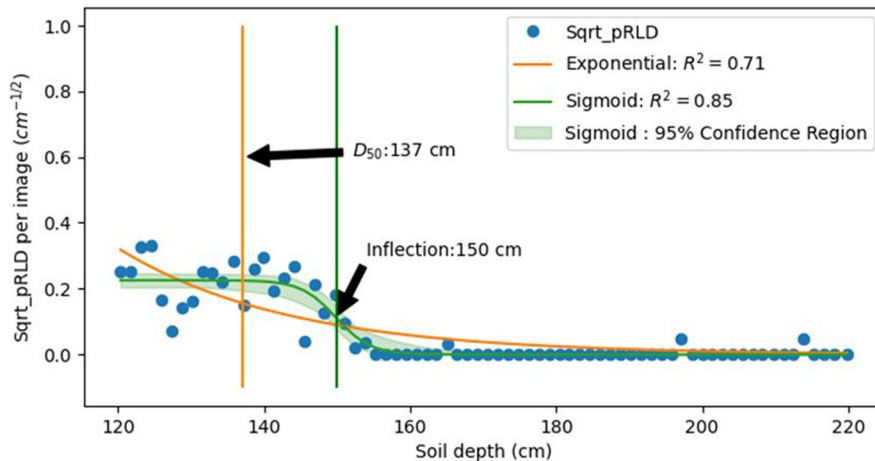


Fig. 2 Square root of planar root length density (Sqrt_pRLD) in a single tube across soil depth in June 2018. The blue dots represent Sqrt_pRLD at every 3.5 cm soil depth. The distribution was modelled using an exponential decay model with D_{50}

at 138 cm (± 2.86 cm) (The SciPy Community 2019) and a sigmoid function with inflection point at 150 cm (± 0.01 cm). The shaded areas represent the 95% confidence region for the sigmoid function

using the “curve_fit” function in the SciPy (Community 2019) optimization library). Specifically, with y being the Sqrt_pRLD at depth x , after fitting the exponential function

$$y = a e^{-bx}, \tag{1}$$

we computed the depth (D_{50} , corresponds to orange line in Fig. 2), at which 50% of the Sqrt_pRLD is accumulated (Fan et al. 2016), as $D_{50} = \log(2)/b$, where a , and b are the parameters of the model.

Similarly, we fitted to the sigmoid function

$$y = \frac{a}{1 + e^{-b(x-c)}} \tag{2}$$

and extracted the sigmoid inflection (SI) (green line in Fig. 2) point c as the estimate of the root depth.

These designed estimates (D_{50} and SI) were calculated of all the tubes and from all three months of root measurements in the datasets from the winter wheat experiments in the years 2018 and 2019.

Root distribution analysis across soil layers

We accumulated the Sqrt_pRLD in 10 intervals in the deeper soil layers between 119 and 220 cm to provide consistent depth data for all months of the two observation years for the machine learning models. The average Sqrt_pRLD across all facility

tubes at different depths from 119 to 220 cm in the two years is illustrated in Fig. 3.

In total from the three observations months (May, June and July), this gives 30 input variables for predicting the outcomes in the form of the isotope measurements (15N or 13C).

Machine learning algorithms

We evaluated alternative ensemble ML algorithms, random forest and gradient boosting, to model the relationship between the Sqrt_pRLD summed into intervals and the isotope tracer measurements. Ensemble learning methods are comprised of a set of classifiers that aggregate predictions to find the estimated results. Boosting and bagging are the two most used families of ensemble methods. The bagging method (e.g. RF) was introduced by Breiman (1996); it is a method of selecting a random sample with replacement of data from a training. In general, bagging is used with weak learners that exhibit high variance and low bias, whereas boosting (e.g. GB (Friedman 2001) is used when low variance and high bias are observed. We have used two alternative ML algorithms (RF and GB) for our analysis and computed also bias-variance of the models (Avati 2019), which are described below in result section.

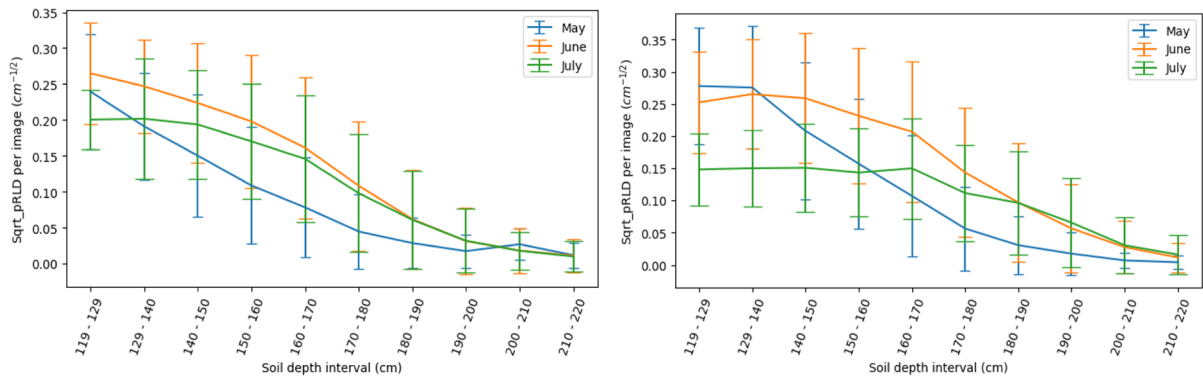


Fig. 3 Average square root of planar root length density (Sqrt_pRLD) across all facility lines accumulated for 10 depth intervals between 119 and 220 cm in 2018 (left) and 2019 (right).

The colors represent the three different imaging time-points. Error bars representing the standard deviation

Random forest

The RF model, introduced by Breiman (2001), is an ensemble learning method aimed at reducing model variance. It is a collection of low correlated decision trees based on the bagging and feature randomness methods. These types of decision trees are also called regression tree if it is used for regression. Regression trees are constructed through the splitting of the data into smaller segments by nodes or branches. The trees in the RF forest model are trained independently, and their outcomes are then averaged. The prediction variance of the RF model is reduced by averaging the model predictions across the trees.

Gradient boosting

The GB model, introduced by Friedman (2001), is a boosting ensemble method. Essentially, the GB model aims at enhancing model accuracy and robustness by aggregating multiple weak learners. Gradient-boosted trees are constructed iteratively as other boosting methods, but they offer the advantage of optimizing an arbitrary differentiable loss function (Friedman 2001), but it generalizes the other machine learning methods by allowing optimization of differentiable loss function.

Statistical analysis

We performed analyses utilizing the identical dataset as the published study by Wacker et al. (2022).

Furthermore, we incorporated additional ^{13}C data obtained from the same experiment to specifically investigate water uptake by deep roots.

The performance of the ML predictions was evaluated using cross-validation. The performance metrics were correlation coefficient (R) and bias-variance in model prediction (Supplementary Table S1) where model estimates were compared to measured ^{15}N uptake and ^{13}C discrimination.

For the RF and GB models, we combined the Sqrt_pRLD estimates for all three months into a single model. The RF and GB models have a number of hyper parameters that may be optimized to the task at hand. For most hyper parameters, we used the default values in the SciKit-Learn (Pedregosa et al. 2011) Python implementation. However, for hyper parameters like number of trees, maximum depth of the trees, and maximum number of features included, we used nested cross-validation to optimize these parameters.

In all cases we tested using five-fold cross validation, the RF models performed slightly better than GB model and for simplicity we only investigated the RF model further for feature importance and mediation analysis. Similarly, we only performed mediation for the SI estimate (and not D_{50}). We computed feature importance to investigate which segment of soil layers are most important for ^{15}N uptake and ^{13}C discrimination. This was quantified by the RF average impurity reduction (Breiman 2001).

Mediation analysis was carried out using the SI (May, June, and July) and RF models for predicting $\log \delta^{15}\text{N}$ and $\delta^{13}\text{C}$ as mediators to determine

the genotype effect (Fig. 4) of deep root traits on $\log \delta^{15}\text{N}$, and $\delta^{13}\text{C}$ using the approach used in Wacker et al. (2022). Using mediation analysis, we can determine how a genotype (ID) and a dependent variable ($\log \delta^{15}\text{N}$ or $\delta^{13}\text{C}$) were related by using a mediator variable.

Result

Sigmoid inflections and Sqrt_pRLD for different months in 2018 and 2019 are summarized in Table 1. There was an average Sqrt_pRLD of 16 $\text{cm}^{-1/2}$ per minihizotron in May, compared to 10 $\text{cm}^{-1/2}$ in June and 6 $\text{cm}^{-1/2}$ in July 2018. June measurements showed a higher average rooting depth (SI) of 171 cm compared to 154 cm in May and 169 cm in July 2018, whereas July measurements showed a higher average rooting depth of 189 cm compared to 163 cm in May and 182 cm in June 2019.

Correlation between root models and isotopes

The correlation coefficients between parametrized models (D_{50} and SI) or ML models (RF and GB) and the isotope measurements ($\log \delta^{15}\text{N}$ and $\delta^{13}\text{C}$) are shown in Table 2. In general, SI had a higher correlation with $\log \delta^{15}\text{N}$ and $\delta^{13}\text{C}$ than D_{50} showing SI to be relevant estimator of rooting depth. The correlation between root-depth estimates and $\log \delta^{15}\text{N}$ was lower in 2019 than in 2018. However, there were no statistically significant correlations with $\delta^{13}\text{C}$ ($p \geq 0.05$) in 2019. In the 2018 experiment, the RF algorithm showed a higher correlation ($R = 0.46$ for $\log \delta^{15}\text{N}$, and $R = 0.41$ for $\delta^{13}\text{C}$) between predicted and observed corrected values of isotopes than the GB ($R=0.42$ for $\log \delta^{15}\text{N}$, and $R = 0.39$ for $\delta^{13}\text{C}$) but in 2019 correlations were not statistically significant ($p \geq 0.05$). The potential reasons for absence of significance in correlation between deep roots and $\delta^{13}\text{C}$ in 2019 are many. In 2018, transpiration demand and water stress were more prominent compared to 2019, due to higher average temperature during growth period (particularly in the late growing season) of

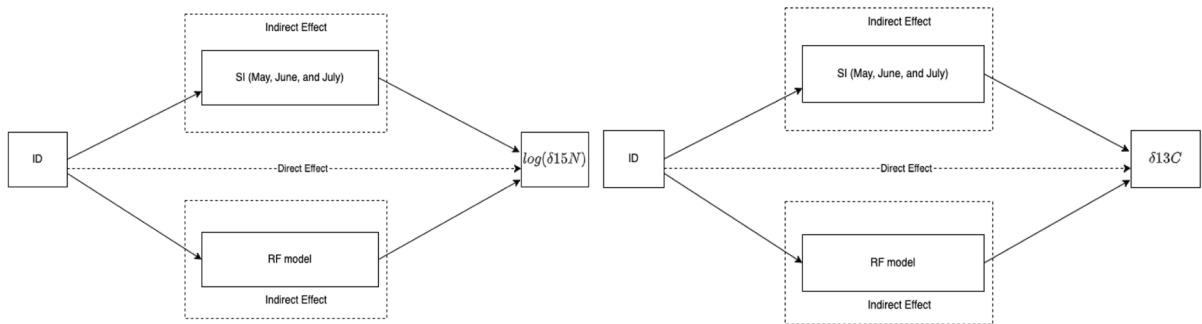


Fig. 4 Path diagram (Hayes 2013) of mediation analysis of the genotypic effect of root traits on ^{15}N uptake (left) and ^{13}C discrimination (right)

Table 1 Summary of Sqrt_pRLD per minihizotron and SI in the 2018 and 2019 dataset, for May, June, and July

Descriptive statistics	Sqrt_pRLD per minihizotron ($\text{cm}^{-1/2}$)						SI (cm)					
	May		June		July		May		June		July	
Year	2018	2019	2018	2019	2018	2019	2018	2019	2018	2019	2018	2019
mean	16	19	10	20	6	14	154	163	171	182	169	189
std	4	4	3	5	3	3	15	14	15	16	16	17
min	0	7	2	7	0	4	111	133	129	117	124	121
max	25	29	19	61	14	22	197	194	214	231	211	228

Table 2 Correlation coefficient (R) with uncertainties (Haukoos and Lewis 2005) between the root-depths estimated by the SI, D₅₀ and the RF and GB model versus the isotope (log δ¹⁵N and δ¹³C) measurements

R		2018		2019	
		logδ ¹⁵ N	δ ¹³ C	logδ ¹⁵ N	δ ¹³ C
D ₅₀	May	0.26 (± 0.05) ***	-0.17 (± 0.06) **	0.17 (± 0.07)*	-0.01 (± 0.08) NS
	June	0.32 (± 0.05) ***	-0.21 (± 0.05) ***	0.17 (± 0.08)*	0.13 (± 0.06) NS
	July	0.31 (± 0.04) ***	-0.18 (± 0.05) **	0.18 (± 0.07)**	0.08 (± 0.06) NS
SI	May	0.34 (± 0.05) ***	-0.27 (± 0.05) ***	0.15 (± 0.07)*	-0.02 (± 0.07) NS
	June	0.37 (± 0.06) ***	-0.30 (± 0.05) ***	0.17 (± 0.07)*	0.06 (± 0.07) NS
	July	0.39 (± 0.05) ***	-0.31 (± 0.04) ***	0.24 (± 0.07)***	0.12 (± 0.07) NS
RF	May + June + July	0.46 (± 0.04) ***	0.41 (± 0.04) ***	0.10 (± 0.06) NS	0.06 (± 0.07) NS
GB	May + June + July	0.42 (± 0.04) ***	0.39 (± 0.05) ***	-0.01 (± 0.07) NS	0.10 (± 0.06) NS

We trained RF and GB models on Sqrt_pRLD data from May, June, and July across 10 intervals using cross-validation. The correlations which were not statistically significant in 2019 are marked with NS ($p \geq 0.05$), * represents $p < 0.05$, ** $p < 0.01$, *** $p < 0.001$

winter wheat, which resulted in higher soil temperature, higher evapotranspiration (ET_o), less water available in the soil, earlier ripening and crops being water stressed. While the subsoil was irrigated in 2018, this did not succeed in alleviating the water stress on the topsoil. This phenomenon has been described before (Rasmussen et al. 2020) and the reasons behind it are still to be better understood. Additionally, in 2018 isotope samples were positioned, so plants (roots) were belonging to the dry part of the facility, while in 2019 due to reverse water stress isotope sample was taken from the part of the facility where plants/roots were less water stressed.

In terms of variance (Supplementary Table S1), the GB model exhibited higher variability in its predictions for log δ¹⁵N and δ¹³C in 2018, with a variance of 0.52, compared to the RF model which had a lower variance of 0.37 for predicting log δ¹⁵N. This suggests that the GB model's predictions might have more fluctuation or dispersion. Moving on to 2019, both models showed slightly higher biases, with the RF model having a bias of -0.04 and the GB model with a slightly larger bias of -0.06. However, when considering variance, the RF model displayed lower variability (0.06) compared to the GB model (0.15) for predicting log δ¹⁵N in the same year. This indicates that the predictions from the RF model were more robust and therefore exhibited less variability compared to the GB model.

Importance of deep roots for 15N uptake and 13C discrimination

The relationship between the root depth, as estimated by the SI model, and the isotopes allows a simple estimation of the importance of deep root function. For instance, the correlation plot of δ¹³C and SI in June 2018 is illustrated in Fig. 5 (top right). The parameters in the regression lines allows a simple interpretation of the impact of deep rooting. From the slopes for the correlation plots against 15N (Fig. 5, top left, and Supplementary Table S2), we can see that if rooting depth increases by 1 cm, then we would expect log δ¹⁵N to be higher on average by 3% (± 0.5%) in June 2018 (dry year) and 1% (± 0.4%) in June 2019. Deep roots play a critical role in the 13C discrimination process, offering valuable insights into our understanding of drought resilience. If the depth of rooting extends by 1 cm (as depicted in Fig. 5, top right and Supplementary Table S2), there would be an average reduction of 1% (± 0.4%) in δ¹³C levels during June 2018, indicated by the negative slope of -0.01. However, during 2019 (as shown in Fig. 5, bottom right), the R² value stands at 0.0 due to the lack of statistically significant correlations between root depth and δ¹³C, as discussed earlier and presented in Table 2.

Importance of root distributions

The feature importance quantification for the RF model allows an interpretation of the importance of Sqrt_pRLD at different depths across the three

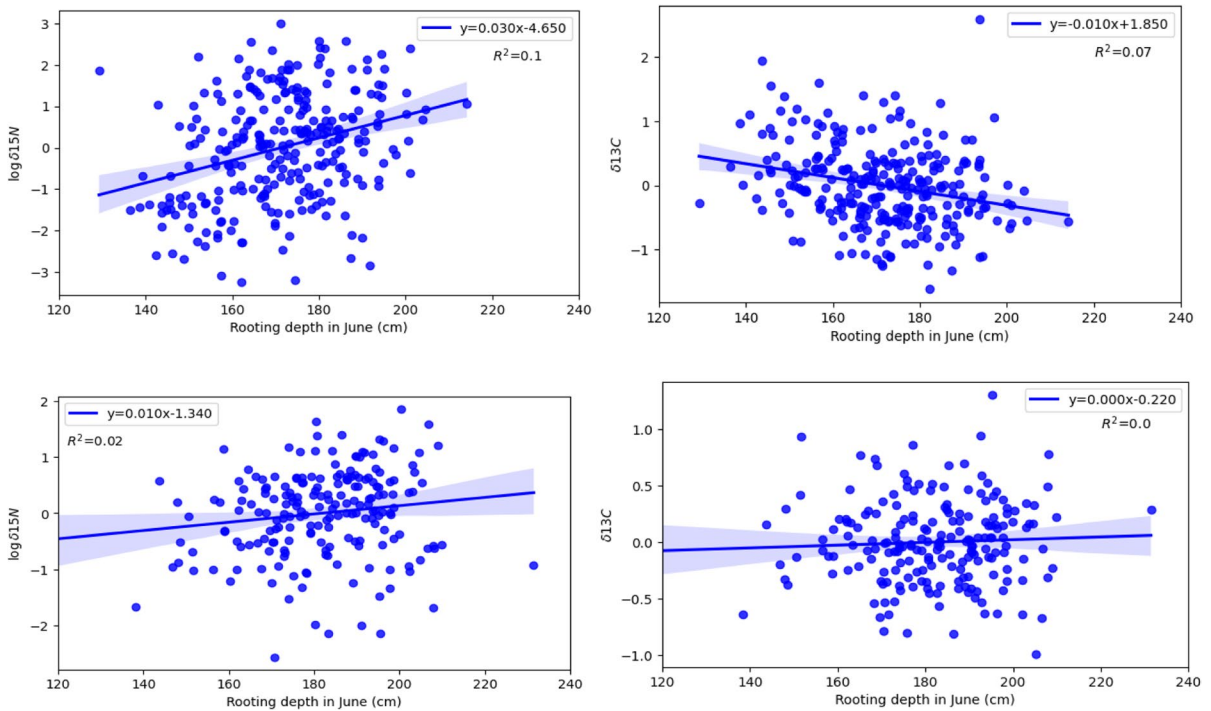


Fig. 5 Deep root functioning analysis using root depth estimated by SI and correlated against isotope measurements. The top row is 2018 and bottom row is 2019. Left is 15N and right is 13C. The Y labels are centred around zero. The shaded areas

represent the 95% confidence intervals for the regression lines, which represent the uncertainty of the regression coefficients. The uncertainties (Lane et al. 2003) of the regression coefficients are provided in Supplementary Table S2

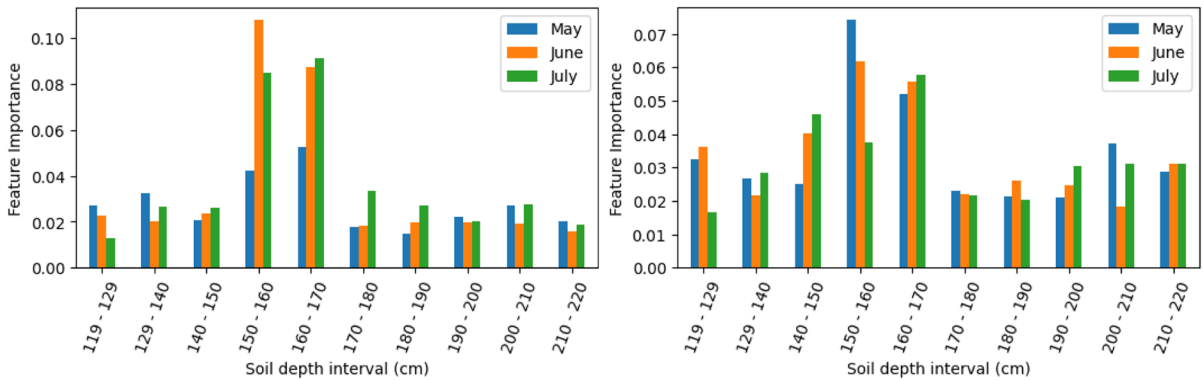


Fig. 6 Random Forest feature importance for 15N uptake (left) and, 13C discrimination (right) in 2018. The feature importance of May, June, and July are plotted against at 10

different soil depth intervals between 119–220 cm to visualize the important depths for 15N uptake and 13C discrimination, respectively

observation months. Figure 6 illustrates this and demonstrates that throughout all three months, Sqrt_pRLD found at depths 150–160 cm and 160–170 cm were the most important features for predicting both 15N and 13C in 2018. Based on the figure, the soil

depth between 150 and 160 cm had a significant impact on 13C discrimination in May 2018. May’s Sqrt_pRLD at 150–160 cm soil depth was most important for predicting δ13C followed by June and July’s. In contrast, at 160–170 cm depth Sqrt_pRLD

from all months showed equally high importance for 13C discrimination. For 15N, June data were the most important, and May data the least important.

The feature importance of RF model in 2019 is not shown in Fig. 6 as correlation between RF's prediction and log $\delta^{15}\text{N}$ (or $\delta^{13}\text{C}$) was not statistically significant (Table 2).

Interplay between genotypes, models, and isotopes

The mediation analysis of both direct and indirect effects of genotype on log $\delta^{15}\text{N}$ and $\delta^{13}\text{C}$ is shown in Tables 3 and 4. In both years, the genotype significantly influenced all deep root estimators and RF models. The genotype effect on individual root depths

Table 3 Mediation analysis of deep rooting on the genotype effect on 15N uptake. R^2 of the total effect and decomposition of R^2 for direct genotype (ID) and indirect effects (May SI, June SI, July SI, and RF model) predicting 15N uptake

Genotype effect on Individual deep root depth and RF model		Significance of parameters of the total effect model		
Year	Parameter	p value	Parameter	p value
2018	May SI	5×10^{-6}	ID	2×10^{-9}
	June SI	4×10^{-7}	May SI	0.27
	July SI	6×10^{-7}	June SI	0.61
	RF Model	6×10^{-4}	July SI	0.52
2019	May SI	1×10^{-5}	RF Model	2×10^{-4}
	June SI	2×10^{-3}	ID	3×10^{-9}
	July SI	3×10^{-3}	May SI	0.60
	RF Model	2×10^{-7}	June SI	0.54
2018	ID	43.4	July SI	0.16
	May SI		RF Model	2×10^{-2}
	June SI			
	July SI			
2019	ID	56.4		
	May SI			
	June SI			
	July SI			
2018	ID	43.4	Percentage due to direct effect	85.8
	May SI		Percentage due to indirect effect	3.1
	June SI			3.7
	July SI			3.2
2019	ID	56.4		5.1
	May SI			
	June SI			
	July SI			
2018	ID	47.4	Percentage due to direct effect	89.1
	May SI		Percentage due to indirect effect	2.7
	June SI			2.5
	July SI			3.4
2019	ID	79.4		2.3
	May SI			
	June SI			
	July SI			
2018	ID	47.4	Percentage due to direct effect	89.1
	May SI		Percentage due to indirect effect	2.7
	June SI			2.5
	July SI			3.4
2019	ID	79.4		2.3
	May SI			
	June SI			
	July SI			
2018	ID	47.4	Percentage due to direct effect	89.1
	May SI		Percentage due to indirect effect	2.7
	June SI			2.5
	July SI			3.4
2019	ID	79.4		2.3
	May SI			
	June SI			
	July SI			
2018	ID	47.4	Percentage due to direct effect	89.1
	May SI		Percentage due to indirect effect	2.7
	June SI			2.5
	July SI			3.4
2019	ID	79.4		2.3
	May SI			
	June SI			
	July SI			

Table 4 Mediation analysis of deep root depths on the genotype effect of 13C discrimination

Genotype effect on Individual deep root depth and RF model			Significance of parameters of the total effect model	
Year	Parameter	p value	Parameter	p value
2018	May SI	5×10^{-6}	ID	8×10^{-15}
	June SI	4×10^{-7}	May SI	0.35
	July SI	6×10^{-7}	June SI	0.31
	RF Model	1×10^{-2}	July SI	0.23
2019	May SI	1×10^{-5}	RF Model	7×10^{-4}
	June SI	2×10^{-3}	ID	2×10^{-16}
	July SI	2×10^{-3}	May SI	5×10^{-2}
	RF Model	3×10^{-5}	June SI	0.37
2018	ID	47.4	July SI	0.81
	May SI		RF Model	0.64
	June SI			
	July SI			
2019	ID	79.4		
	May SI			
	June SI			
	July SI			

R^2 of the total effect and decomposition of R^2 for direct genotype (ID) and indirect effects (May SI, June SI, July SI, and RF model) predicting 13C discrimination

(SI) in May, June and July was statistically significant ($p < 0.05$) in the year 2018. The combined RF model explained 43.4% of the variation in log $\delta^{15}\text{N}$ and 47.4% of the variation in $\delta^{13}\text{C}$ in 2018, and 56.4% of the variation in log $\delta^{15}\text{N}$ and 79.4% of the variation in $\delta^{13}\text{C}$ in 2019.

A significant effect of genotype on both 15N uptake and 13C discrimination was mediated by RF estimators in both years. The indirect effects of rooting depth determined as SI in May, June, and July explained 3.1%, 3.7%, and 3.2% of the variation in 2018, whereas the RF model explained 5.1% of the variation of 15N uptake. Based on the indirect effects of SI in May, June, and July, 2.7%,

2.5%, and 3.4% of the variation of ^{13}C discrimination was explained, respectively, while 2.3% was explained by the RF model. In 2019, according to the indirect effects of SI in May, June, and July, 1.5%, 1%, and 3.3% of the variation of ^{15}N could be explained by SI.

Discussion

The purpose of the study was to confirm the importance of deep rooting as observed before (Wacker et al. 2022), but also to further investigate whether machine learning methods can reveal additional insight into the importance of root distribution across depths.

In particular, we used root images and ^{15}N isotope data from both the 2018 and 2019 wheat experiments, similar to Wacker et al. 2022. In addition, we utilized ^{13}C data in our analysis, and estimated root depth using a sigmoid inflection method. Our study also includes the application of machine learning models to predict isotopes and identify the soil regions that significantly contribute to isotope uptake, specifically using the RF forest algorithm. Finally, we wished to investigate the interplay between wheat genotypes, root growth, and root function.

Is estimated root depth related to water and nitrogen uptake?

We proposed a novel model using the SI as the estimate for deep rooting. This gives a more directly intuitive depth estimate compared to the D_{50} estimate in the previously proposed exponential decay model (Fan et al. 2016). In addition, the SI model fitted the Sqrt_pRLD distribution better (illustrated in Fig. 2). The results demonstrated that the SI root depth estimate was also better at explaining the deep root function measured by ^{15}N and ^{13}C isotope measurements than the exponential model (Table 2). These results confirmed the importance of deep root growth.

The correlations for the SI versus $\log \delta^{15}\text{N}$ were positive, while correlations to $\delta^{13}\text{C}$ were negative. This confirms that increased deep rooting allowed higher uptake of ^{15}N applied deep in the soil, and indirectly, that it also allowed higher water uptake from deep soil layers. The negative correlations of SI with $\delta^{13}\text{C}$ indicates that there was a positive relationship between root depth estimated as SI and drought resilience (Simelton et al. 2009), as deep water uptake allows the plants to

keep their stomata more open. According to the regression lines, if root depth increases by 1 cm, $\log \delta^{15}\text{N}$ will increase by 3% ($\pm 0.5\%$) (Lindeman 1980; Kasza and Wolfe 2014) in June 2018, and if rooting depth increases by 1 cm, $\delta^{13}\text{C}$ will be lower on average by 1% ($\pm 0.4\%$) (slope was -0.01) in June 2018. However, in 2019, correlations between root depth and $\delta^{13}\text{C}$ were not statistically significant (Table 2).

The SI root depth estimate may allow improved estimates of root growth and ability for deep soil exploitation (Burrige et al. 2017). Apart from the rooting depth achieved, also the timing of deep root growth may differ among winter wheat genotypes (Hodgkinson et al. 2017), and this can be significant for resource uptake. Different timing of root growth can be computed by finding the inflection points in June, July, and August on Sqrt_pRLD. Further development in root imaging and image analysis may also directly allow the observation of late root season root growth, which can be of special importance for water and nitrogen uptake during the yield forming growth stages of flowering and grain filling.

Does Sqrt_pRLD distribution across soil depths add additional understanding of root function?

To investigate whether machine learning could provide stronger models for explaining root function, we evaluated the two ensemble models, RF and GB. Here, the RF model showed a higher correlation between root data and isotope tracer measurements (see Table 2), and this was in most cases also higher than analysis based on the SI root depth estimate. Thereby, the RF could potentially reveal additional insight into root function. The RF feature importance visualization (Fig. 6) showed that roots between 150 and 170 cm were most important for explaining isotope tracer measurements. We can see in Table 1 that this interval was actually very similar to the root depth as estimated by SI.

As ^{15}N was injected specifically at 180 cm soil depth, it is encouraging but not surprising, to find that roots at the depth between 150 and 170 cm were the most important for predicting ^{15}N uptake. However, the ^{13}C results are based on general plant water stress response, not on tracers added to a specific depth. Finding that also ^{13}C results are mainly predicted by root data from 150 to 170 cm depth, confirm a more general hypothesis that the deepest part of the root system is crucial for genotype differences in water uptake (Thorup-Kristensen and Kirkegaard, 2016). Crops

primarily extract water from the upper soil layers, where root densities are high and water uptake occurs over an extended period. Therefore, the growth of roots typically does not pose a constraint on water uptake from these upper layers. However, in deep soil layers, there are fewer roots, and roots firstly appear there late in the growing season, providing the chance for using these water resources in the summer when there is not so much water available in the shallow soil layers. In a soil layer where root growth and duration limits the water use, genotypic differences become important for actual water use. This was also found by Kirkegaard (Kirkegaard et al. 2007), who established that the extra water assimilated from deep layers was of extra value for yield production, as it is taken up late during the grain filling phase (Lilley and Kirkegaard 2011).

The SI estimates (Table 2) and the RF feature importance analysis revealed additional effects (Fig. 6). The shift of soil depths important for 15N uptake in 2018, from 150 to 160 cm soil depth in Jun to 160–170 cm soil depth in July indicates continuous root growth post-anthesis to be important for tracer uptake, which was injected at anthesis. During May 2018, soil depths of 150–160 cm contributed significantly to 13C discrimination in grain, while root length at 160–170 cm depth in July, followed by June and May, was the most important factor for 13C discrimination. This again implies a continuously developing root profile over time.

As 15N was not applied until anthesis, and 13C was also measured in grain, produced mainly by post anthesis photosynthesis, roots in May will have had little or no direct influence on the isotopic results. However, root observations in May may be predictive of later root presence and development. Young roots are more easily identified on root images than older roots, as can be seen by the declining root observations in many soil layers from May to June to July. Therefore, roots observed in May may give a relatively good estimate of the roots which will be present later in June and July, when the actual isotopic signatures are created by deep water and 15N uptake.

What is the genotypic contribution to the variation in root growth and function?

We investigated the interplay between genotype and the proposed root models in the mediation analysis. The results (in Tables 3 and 4) showed that as expected the genotype was strongly related to the

isotope tracer measurements. However, for both years and both isotopes, the mediation analysis also demonstrated that both the SI root depth estimate, and the RF model contributed with additional, independent information. This supports that these root models can support plant breeding by explaining root function.

The mediation analysis provides insight into the deep root functions of crops. By establishing a causal chain from genotype to deep root traits to phenotype, mediation analysis provides explicit hypotheses for further functional exploration (Yang et al. 2022). Moreover, the greater direct effect of genotype on 15N uptake, and 13C discrimination in 2018 and 2019 than on the other mediator variables suggests that additional genotypic traits besides the ones recorded by image-based root data influenced 15N uptake and 13C discrimination (Wacker et al. 2022).

Comparison of the model performances

In combination, these results demonstrate the importance of the deep roots, as opposed to, for instance, higher root density in upper soil layers, as the RF model confirmed the importance of root growth at more than 150 cm depth. However, the RF did still achieve higher correlations for most outcomes in Table 2, indicating that some information was lost in the simple calculation of a root depth estimate by the SI model. It is possible that the RF model did in fact implicitly also just estimate the root depth, but became more robust by integrating Sqrt_pRLD measurements from all three months (May, June, and July) as opposed to the SI model that estimated these individually. To investigate this, we create models integrating the three SI estimates using either RF or GB for the combination. These models did not perform better than the individual SI estimates (results not shown). We interpret this to conclude that the RF model using all root data points, does indeed capture more than just root depth, and integrates relevant root characteristics across depths. Although all roots contribute to water uptake, but mainly the deep roots contribute to the variation in water and N uptake.

Conclusions

Our study proposed a novel estimate of root depth by the sigmoid fitted to Sqrt_pRLD measurements across depths. This SI root depth estimate improved the

prediction of root function as investigated by the stable isotopes ^{15}N and ^{13}C . The importance of the deep roots was further confirmed by the RF forest machine learning model that optimally integrated Sqrt_pRLD across depths into a single model. This RF model was slightly better than the SI estimator at explaining isotope tracer measurements, and the RF feature importance analysis revealed that this was achieved with a strong focus on the deepest roots. Further, the mediation analysis showed that both the SI and RF models provided additional information on top of the genotype, showing a potential for applying these in plant breeding experiments. The results are not directly useful for breeders. However, it demonstrates the importance of deep root growth and soil resource uptake and presents a method for phenotyping these traits. This information suggests that breeding programs can utilize these traits to improve genotypes.

Funding Open access funding provided by Royal Library, Copenhagen University Library.

Code and data availability Codes and data are available on GitHub at <https://github.com/satyasaran/CropML.git>.

Declarations

Conflict of interest The authors declare no conflict of interest.

Open Access This article is licensed under a Creative Commons Attribution 4.0 International License, which permits use, sharing, adaptation, distribution and reproduction in any medium or format, as long as you give appropriate credit to the original author(s) and the source, provide a link to the Creative Commons licence, and indicate if changes were made. The images or other third party material in this article are included in the article's Creative Commons licence, unless indicated otherwise in a credit line to the material. If material is not included in the article's Creative Commons licence and your intended use is not permitted by statutory regulation or exceeds the permitted use, you will need to obtain permission directly from the copyright holder. To view a copy of this licence, visit <http://creativecommons.org/licenses/by/4.0/>.

References

- Avati A (2019) Bias-variance analysis: theory and practice. Stanford University. Available at. <http://cs229.stanford.edu/summer2019>. Accessed 21 Jun 2023
- Awika HO, Mishra AK, Gill H, Awika HO, Mishra AK, Gill H, DiPiazza J, Avila CA, Joshi V (2021) Selection of nitrogen responsive root architectural traits in spinach using machine learning and genetic correlations. *Sci Rep* 11:9536. <https://doi.org/10.1038/s41598-021-87870-z>
- Baker RE, Pena J-M, Jayamohan J, Jérusalem A (2018) Mechanistic models versus machine learning, a fight worth fighting for the biological community? *Biol Lett* 14:20170660. <https://doi.org/10.1098/rsbl.2017.0660>
- Breiman L (2001) Random forests. *Mach Learn* 45:5–32. <https://doi.org/10.1023/A:1010933404324>
- Breiman L (1996) Bagging predictors. *Mach Learn* 24:123–40. <https://doi.org/10.1007/BF00058655>
- Burridge JD, Schneider HM, Huynh B-L, Burridge JD, Schneider HM, Huynh B-L, Roberts PA, Bucksch A, Lynch JP (2017) Genome-wide association mapping and agronomic impact of cowpea root architecture. *Theor Appl Genet* 130:419–431. <https://doi.org/10.1007/s00122-016-2823-y>
- Cai G, Vanderborcht J, Klotzsche A, Cai G, Vanderborcht J, Klotzsche A, van der Kruk J, Neumann J, Hermes N, Vereecken H (2016) Construction of minirhizotron facilities for investigating root zone processes. *Vadose Zone J* 15:vzj2016.05.0043. <https://doi.org/10.2136/vzj2016.05.0043>
- Eberbach PL, Hoffmann J, Moroni SJ et al (2013) Rhizolysimetry: facilities for the simultaneous study of root behaviour and resource use by agricultural crop and pasture systems. *Plant Methods* 9:1–19. <https://doi.org/10.1098/rsbl.2017.0660>
- Fan J, McConkey B, Wang H, Janzen H (2016) Root distribution by depth for temperate agricultural crops. *Field Crop Res* 189:68–74. <https://doi.org/10.1016/j.fcr.2016.02.013>
- Friedman JH (2001) Greedy function approximation: a gradient boosting machine. *Ann Stat* 1189–1232. <https://doi.org/10.1214/aos/1013203451>
- Han E, Smith AG, Kemper R, Han E, Smith AG, Kemper R, White R, Kirkegaard JA, Thorup-Kristensen K, Athmann M (2021) Digging roots is easier with AI. *J Exp Bot* 72:4680–4690. <https://doi.org/10.1093/jxb/erab174>
- Haukoos JS, Lewis RJ (2005) Advanced statistics: bootstrapping confidence intervals for statistics with difficult distributions. *Acad Emerg Med* 12:360–365
- Hayes AF (2013) Introduction to mediation, moderation, and conditional process analysis. Guilford Press, New York, NY
- Hodgkinson L, Dodd IC, Binley A, Hodgkinson L, Dodd IC, Binley A, Ashton RW, White RP, Watts CW, Whalley WR (2017) Root growth in field-grown winter wheat: some effects of soil conditions, season and genotype. *Eur J Agron* 91:74–83. <https://doi.org/10.1016/j.eja.2017.09.014>
- Ishwaran H (2007) Variable importance in binary regression trees and forests. *Electron J Stat* 1:519–537. <https://doi.org/10.1214/07-EJS039>
- Kasza J, Wolfe R (2014) Interpretation of commonly used statistical regression models. *Respirology* 19:14–21. <https://doi.org/10.1111/resp.12221>
- Kiranyaz S, Malik J, Abdallah HB, Ince T, Iosifidis A, Gabbouj M (2021) Self-organized operational neural networks with generative neurons. *Neur Netw* 140:294–308. <https://doi.org/10.1016/j.neunet.2021.02.028>
- Kirkegaard JA, Lilley JM, Howe GN, Graham JM (2007) Impact of subsoil water use on wheat yield. *Aust J Agric Res* 58:303–315. <https://doi.org/10.1071/AR06285>

- Lane D, Scott D, Hebl M, Guerra R, Osherson D, Zimmer H (2003) Introduction to statistics. David Lane
- Lilley JM, Kirkegaard JA (2011) Benefits of increased soil exploration by wheat roots. *Field Crop Res* 122:118–130. <https://doi.org/10.1016/j.fcr.2011.03.010>
- Lindeman RH, Merenda PF, Gold RZ (1980) Introduction to bivariate and multivariate analysis. Glenview, IL: Scott, Foresman and company 119
- Pachepsky YA, Rawls WJ (1999) Accuracy and reliability of pedotransfer functions as affected by grouping soils. *Soil Sci Soc Am J* 63:1748–1757. <https://doi.org/10.2136/sssaj1999.6361748x>
- Pedregosa F, Varoquaux G, Gramfort A et al (2011) Scikit-learn: machine learning in Python. *J Mach Learn Res* 12:2825–2830
- Rasmussen CR, Thorup-Kristensen K, Dresbøll DB (2020) Uptake of subsoil water below 2 m fails to alleviate drought response in deep-rooted chicory (*Cichorium intybus* L). *Plant Soil* 446:275–290
- Schaap MG, Leij FJ (1998) Using neural networks to predict soil water retention and soil hydraulic conductivity. *Soil Tillage Res* 47:37–42. [https://doi.org/10.1016/s0167-1987\(98\)00070-1](https://doi.org/10.1016/s0167-1987(98)00070-1)
- Simelton E, Fraser ED, Termansen M et al (2009) Typologies of crop-drought vulnerability: an empirical analysis of the socio-economic factors that influence the sensitivity and resilience to drought of three major food crops in China (1961–2001). *Environ Sci Policy* 12:438–452. <https://doi.org/10.1016/j.envsci.2008.11.005>
- Smith AG, Han E, Petersen J, Smith AG, Han E, Petersen J, Olsen NAF, Giese C, Athmann M, Dresbøll DB, Thorup-Kristensen K (2022) RootPainter: deep learning segmentation of biological images with corrective annotation. *New Phytol* 236:774–791. <https://doi.org/10.1111/nph.18387>
- Smith AG, Petersen J, Selvan R, Rasmussen CR (2020) Segmentation of roots in soil with U-Net. *Plant Methods* 16:1–15. <https://doi.org/10.1186/s13007-020-0563-0>
- Strobl C, Boulesteix A-L, Zeileis A, Hothorn T (2007) Bias in random forest variable importance measures: illustrations, sources and a solution. *BMC Bioinformatics* 8:1–21. <https://doi.org/10.1186/1471-2105-8-25>
- Svane SF, Dam EB, Carstensen JM, Thorup-Kristensen K (2019a) A multispectral camera system for automated minirhizotron image analysis. *Plant Soil* 441:657–672. <https://doi.org/10.1007/s11104-019-04132-8>
- Svane SF, Jensen CS, Thorup-Kristensen K (2019b) Construction of a large-scale semi-field facility to study genotypic differences in deep root growth and resources acquisition. *Plant Methods* 15:1–16. <https://doi.org/10.1186/s13007-019-0409-9>
- The SciPy Community (2019) SciPy documentation—Scipy.optimize.curve_fit; The SciPy Community, Available online: https://docs.scipy.org/doc/scipy/reference/generated/scipy.optimize.curve_fit.html. Accessed 7 Mar 2022
- Thorup-Kristensen K, Kirkegaard J (2016) Root system-based limits to agricultural productivity and efficiency: the farming systems context. *Ann Botany* 118:573–592. <https://doi.org/10.1093/aob/mcw122>
- Toms BA, Barnes EA, Ebert-Uphoff I (2020) Physically interpretable neural networks for the geosciences: applications to earth system variability. *J Adv Model Earth Syst* 12. <https://doi.org/10.1029/2019MS002002>
- Wacker TS, Popovic O, Olsen NA et al (2022) Semifield root phenotyping: Root traits for deep nitrate uptake. *Plant Cell Environ* 45:823–836. <https://doi.org/10.1111/pce.14227>
- Yang Z, Xu G, Zhang Q, Yang Z, Xu G, Zhang Qi, Obata T, Yang J (2022) Genome-wide mediation analysis: an empirical study to connect phenotype with genotype via intermediate transcriptomic data in maize. *Genetics* 221:iyac057. <https://doi.org/10.1093/genetics/iyac057>
- Zhang Y, Tobias HJ, Brenna JT (2009) Steroid isotopic standards for gas chromatography-combustion isotope ratio mass spectrometry (GCC-IRMS). *Steroids* 74:369–378. <https://doi.org/10.1016/j.steroids.2008.10.001>
- Zuo Q, Jie F, Zhang R, Meng L (2004) A generalized function of wheat's root length density distributions. *Vadose Zone J* 3:271–277. <https://doi.org/10.2113/3.1.271>

Publisher's Note Springer Nature remains neutral with regard to jurisdictional claims in published maps and institutional affiliations.